NATURAL GAS PRICES AND THE EXTREME WINTERS OF 2011/12 AND 2013/14

Causes, Indicators, and Interactions

BY CARL J. SCHRECK III, STEPHEN BENNETT, JASON M. CORDEIRA, JAKE CROUCH, JENNY DISSEN, ANDREA L. LANG, DAVID MARGOLIN, ADAM O'SHAY, JARED RENNIE, THOMAS IAN SCHNEIDER, AND MICHAEL J. VENTRICE

Volatility in the natural gas markets can be linked to large temperature variability over the United States in recent winters.

Natural gas is one of the primary sources of energy in the United States. About half of the nation's households use natural gas to heat their homes (U.S. Energy Information Administration 2012). Commodity prices for natural gas become particularly volatile during the peak heating months of December–February, when temperature fluctuations can have large impacts on heating demand. The sensitivity of natural gas markets to weather was unmistakable in the winters of 2011/12 and 2013/14. Unusually warm temperatures in 2011/12 suppressed demand and drove natural gas prices downward, whereas the reverse happened in 2013/14. This study will examine the relationship between weather and natural gas during these two winters. We will use these examples to illustrate how energy meteorologists and traders use weather and climate data to inform their actions in the market.

Natural gas is traded as a commodity on both the Chicago Mercantile Exchange (CME) and the Intercontinental Exchange (ICE). Although numerous natural gas contracts exist, the most common is the Henry Hub natural gas price. Henry Hub is a major pipeline junction in Louisiana, and the quoted price is that of delivery at the hub in terms of dollars per million British thermal units (mmBTU). One mmBTU is equivalent to about 1000 cubic feet (28.3 m^3) of natural gas and is enough to heat an average home for 4 days. The prices quoted in this study will be Henry Hub futures contracts with the earliest delivery date (i.e., the price for delivery in the calendar month following the trade date). Natural gas producers trade futures contracts of Henry Hub natural gas to hedge their risk against market volatility from weather-driven fluctuations in demand. Many traders also speculate in the market to profit from market inefficiencies.

Numerous forces impact the price of natural gas on a variety of different time scales. For example, the advent of high-volume hydraulic fracturing has significantly increased the available supply of natural gas (Turcotte et al. 2014). This increased supply has driven prices downward, although it has been constrained somewhat by the lack of new pipelines to deliver the supply to consumers (Philips 2014). Another external force on the market is the interplay between prices for natural gas and other energy sources (Mjelde and Bessler 2009; Joëts and Mignon 2012; Pettersson et al. 2012). Many electricity companies have the ability to change their production portfolio as seasonal prices fluctuate. The recent drop in natural gas prices has made natural gas more competitive with coal,

oil, and nuclear energy for electricity production. As a result, more utilities are using natural gas to produce electricity and retiring plants that use other fuels (U.S. Energy Information Administration 2012). This "gas for power burn" naturally increases demand for natural gas until the price rises to equilibrium with other fuels.

The largest day-to-day volatility in natural gas prices has been weather-driven demand, which varies by season and region (Linn and Zhu 2004; Mu 2007; Brown and Yücel 2008). The shift toward natural gas as an electricity source has also increased the sensitivity of prices to summer temperatures in the southeastern and south-central United States. However, the greatest weather-related sensitivity still occurs during December–February. During winter, natural gas prices are sensitive to temperatures in the northeastern quadrant of the country roughly bounded by Chicago, Illinois; Boston, Massachusetts; and Atlanta, Georgia (Fig. 1), commonly referred to in the industry as the Midwest–East or the consuming East.

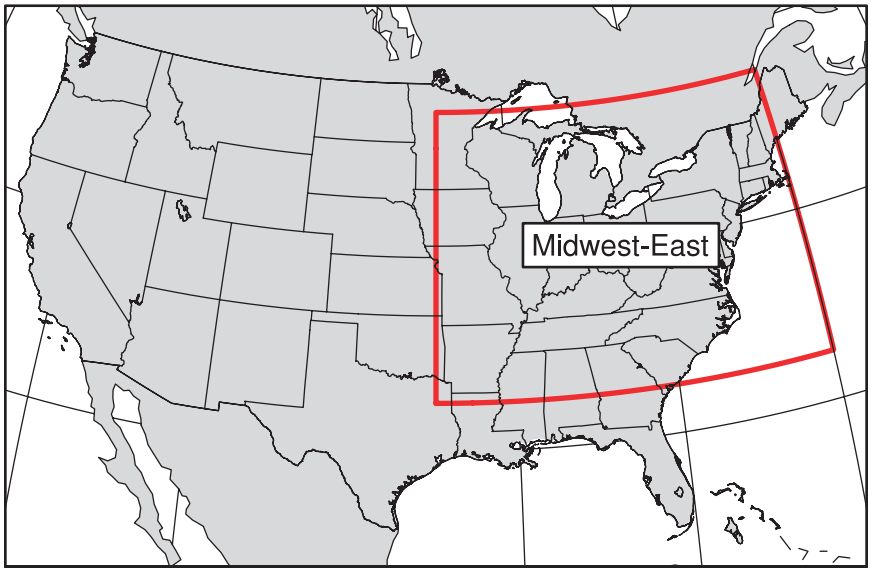

Fig. 1. Outline of the Midwest–East region used in this study to focus on the region where temperatures have the greatest effect on natural gas demand.

Many traders are particularly interested in temperature forecasts at horizons of 2–4 weeks. Monthly futures contracts are naturally forward looking, as they are related to the actual or "spot" price of natural gas weeks or even months later. Weeks 2–4 are also critical time scales for natural gas producers. They can adjust their drilling operations and the prices for natural gas from the wellhead into the pipelines based on the anticipated demand 2–4 weeks later, when that natural gas will be consumed.

Forecasts from global dynamical models play a major role in the natural gas markets. These forecasts are widely available either directly from the forecast centers or through numerous weather vendors (i.e., private companies), so the markets respond quickly to how the forecast temperatures would influence natural gas demand. Large fluctuations in price can happen when the temperature forecast, especially for days 6–15, changes significantly from one model run to the next. The price of natural gas is often most volatile when the 1200 UTC forecast models are released. That is the only model cycle that is disseminated while the markets are open. Traders watch and react as each model run is released: the National Centers for Environmental Prediction (NCEP) Global Forecast System (GFS) at around 1015 eastern standard time (EST), the NCEP Global Ensemble Forecast System (GEFS) at around 1045 EST, and the European Centre

AFFILIATIONS: Schreck, Dissen, and Rennie—Cooperative Institute for Climate and Satellites—North Carolina, North Carolina State University, and NOAA/National Centers for Environmental Information, Asheville, North Carolina; Bennett—EarthRisk Technologies, San Diego, and Verisk Climate, San Francisco, California; Cordeira—Department of Atmospheric Science and Chemistry, Plymouth State University, Plymouth, New Hampshire; Crouch—NOAA/National Centers for Environmental Information, Asheville, North Carolina; Lang—Department of Atmospheric and Environmental Sciences, University at Albany, State University of New York, Albany, New York; Margolin—EarthRisk Technologies, San Diego, California; O'Shay—EarthRisk Technologies, San Diego, California, and Leeward Pointe Capital, Austin, Texas; Schneider—Boston College, Boston, Massachusetts; Ventrice—Weather Service International, Andover, Massachusetts
CORRESPONDING AUTHOR: Carl J. Schreck III, Cooperative Institute for Climate and Satellites—NC, 151 Patton Ave., Asheville, NC 28801
E-mail: cjschrec@ncsu.edu

The abstract for this article can be found in this issue, following the table of contents.

DOI:10.1175/BAMS-D-13-00237.1

In final form 25 November 2014

for Medium-Range Weather Forecasts (ECMWF) deterministic model at around 1400 EST. Speed is crucial to weather vendors that provide these forecasts to traders because prices react as each individual forecast hour is released for a given model. If one vendor can anticipate or distribute those forecasts faster than other sources, then their clients can profit by making their stance in the market before others have access to that information.

Dynamical model forecasts have limited skill beyond 1–2 weeks (Hagedorn et al. 2008; Saha et al. 2006, 2014), but longer-range forecasts are still priced into the market. Savvy traders can profit if they have access to better forecasts because the market will move toward the observed temperatures as the lead-time decreases. Traders often work with energy meteorologists since human forecasts are generally more skillful than those from dynamical models (Roebber and Bosart 1996; Novak et al. 2014). The improvement in skill comes from a combination of forecaster experience and leveraging teleconnections, especially from the tropics and the Arctic. Teleconnections represent low-frequency systems that have life cycles extending beyond the predictive skill of many models (Van Oldenborgh et al. 2003; Saha et al. 2006). Energy meteorologists use the current states of these teleconnections in statistical models or simply examine composite temperature anomalies based on analogous past events. Comparing these composites with the dynamical model forecasts is one way that meteorologists estimate the reliability of those forecasts. A critical component for making these composites or statistical models is having access to datasets like NOAA's climate data records (National Research Council 2004), which are long enough to identify a large sample of past events and also have sufficient homogeneity to ensure data consistency between those events. The primary tropical teleconnections are the El Niño–Southern Oscillation (ENSO) and the Madden–Julian oscillation (MJO). Key Arctic teleconnections include the Arctic Oscillation (AO), the North Atlantic Oscillation (NAO), Eurasian snow cover, and stratospheric temperature and wind anomalies.

ARCTIC TELECONNECTIONS. Two of the leading modes of low-frequency variability in the Northern Hemisphere circulation are the AO and the NAO (Barnston and Livezey 1987). These modes are correlated with each other (Thompson and Wallace 1998; Ambaum et al. 2001), and they are also both positively correlated with Midwest–East temperatures (Higgins et al. 2000, 2002). The AO is related to the strength and orientation of the circumpolar jet. When the AO is positive, the jet is stronger and more zonal, which confines the coldest air to the

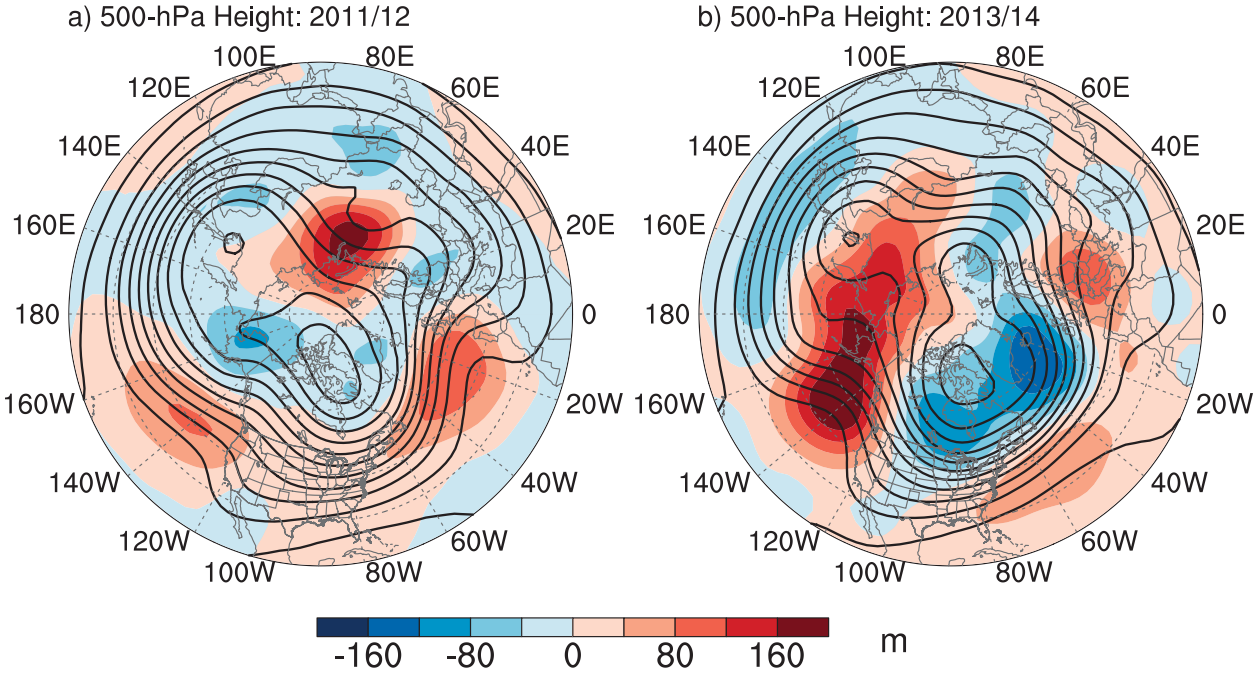

Fig. 2. NCEP–Department of Energy (DOE) Reanalysis-2 (Kanamitsu et al. 2002) 500-hPa geopotential heights (contours) and anomalies relative to 1981–2010 for Dec–Feb (a) 2011/12 and (b) 2013/14. Contours are drawn every 80 m.

Arctic region. Conversely, negative AO is associated with higher-amplitude waves in the jet and generally colder temperatures over the Midwest–East. The NAO is related to the strength and location of the jet and the extratropical storm track over the North Atlantic (Hurrell et al. 2003). Negative AO indicates colder temperatures and more frequent winter storms over the Midwest–East.

Figure 2 shows the mean 500-hPa geopotential heights and anomalies from climatology for December–February 2011/12 and 2013/14. The pattern for 2011/12 was a classic positive AO (Fig. 2a) with negative anomalies near the pole, positive anomalies in the midlatitudes, and a generally zonal flow across the Western Hemisphere. This pattern would be consistent with an extension of the jet over the eastern North Pacific, which limits the opportunities for Arctic intrusions into the United States. Figure 2b shows a very different pattern in 2013/14. Positive anomalies greater than 200 m over the Gulf of Alaska disrupt the eastward extension of the Pacific jet. The ridging associated with these anomalies extended northward all the way to the pole and was associated with enhanced troughing of the central portions of Canada and the United States. The resulting cross-polar flow transported cold Siberian air into the Midwest–East region.

Energy meteorologists often look for ways to forecast changes in the AO and the NAO because of their large impact on Midwest–East temperatures. The stratosphere provides one such source of predictability (Thompson and Wallace 1998; Baldwin and Dunkerton 1999, 2001; Black 2002; Gerber et al. 2012). The stratosphere has a long memory, which makes it useful for long-range forecasting (Newman and Rosenfield 1997; Baldwin et al. 2003; Gerber et al. 2012). Variations in the stratospheric polar vortex can be observed on average 3 weeks before they propagate downward and manifest themselves in the troposphere (Thompson and Wallace 1998; Baldwin and Dunkerton 1999, 2001; Black 2002; Gerber et al. 2012). Accurate representation of the stratosphere also plays a role in the skill of dynamical models (Tripathi et al. 2014). Initialization differences in the stratosphere can affect tropospheric forecasts at leads as short as a few days (Charlton et al. 2004; Jung and Barkmeijer 2006; Gerber et al. 2012). Conversely, improvements to model forecasts of the stratosphere can improve the tropospheric skill for forecasts as long as 3–4 weeks (Roff et al. 2011).

Sudden stratospheric warming (SSW) is a notable exception to the stratosphere's otherwise slow evolution. About every other year, the Northern Hemisphere stratospheric polar vortex abruptly

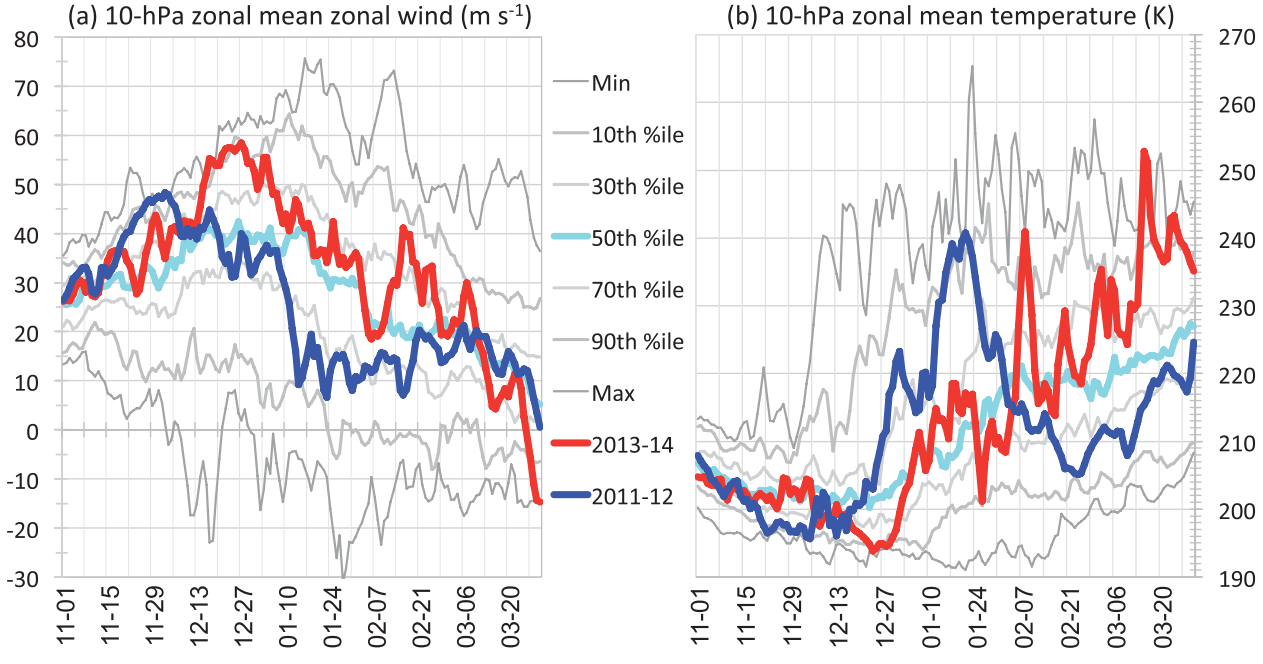

Fig. 3. For the winter (Nov–Mar) of 2011/12 (blue) and 2013/14 (red) along with the minimum, maximum, and 10th, 30th, 50th, 70th, and 90th percentiles for the period covering 1978/79–2013/14, (a) the 10-hPa zonal-mean zonal wind (m s^{-1}) at 60°N and (b) the 10-hPa zonal temperature (K) at 80°N. Data from the National Aeronautics and Space Administration (NASA) Modern-Era Retrospective Analysis for Research and Applications (MERRA; Rienecker et al. 2011).

weakens and the stratosphere dramatically warms (Labitzke 1972; Gerber et al. 2012). These SSWs typically lead to negative AO conditions in the troposphere that can persist for up to 2 months and are associated with persistent cold anomalies over the Midwest–East (Baldwin and Dunkerton 2001; Thompson and Wallace 2001; Thompson et al. 2002).

Figure 3 shows two zonal-mean diagnostics of the stratospheric polar vortex, 10-hPa zonal wind and temperature, during November–March 2011/12 and 2013/14. Both years experienced increases in high-latitude 10-hPa temperatures that coincided with weakening of the 10-hPa westerlies. These warming events did not meet the World Meteorological Organization (WMO) criteria for a major SSW because the zonal-mean circulation never reversed sign from westerly to easterly. However, the stratosphere does not need to experience a major SSW for stratospheric thermal and wind anomalies to impact the tropospheric circulation (Tripathi et al. 2014). For example, the 10-hPa zonal wind rapidly decelerated from over 35 to less than 10 m s^{-1} during the first week of January 2012. Consistent with previous studies (Thompson and Wallace 1998; Baldwin and Dunkerton 1999, 2001; Black 2002; Gerber et al. 2012), this stratospheric warming was associated with a shift in the tropospheric AO index from +2.2 in December 2011 to −0.2 in January 2012 (Fig. 8c).

Despite the zonal-mean similarities in 2011/12 and 2013/14 (Fig. 3), the two winters exhibited notably

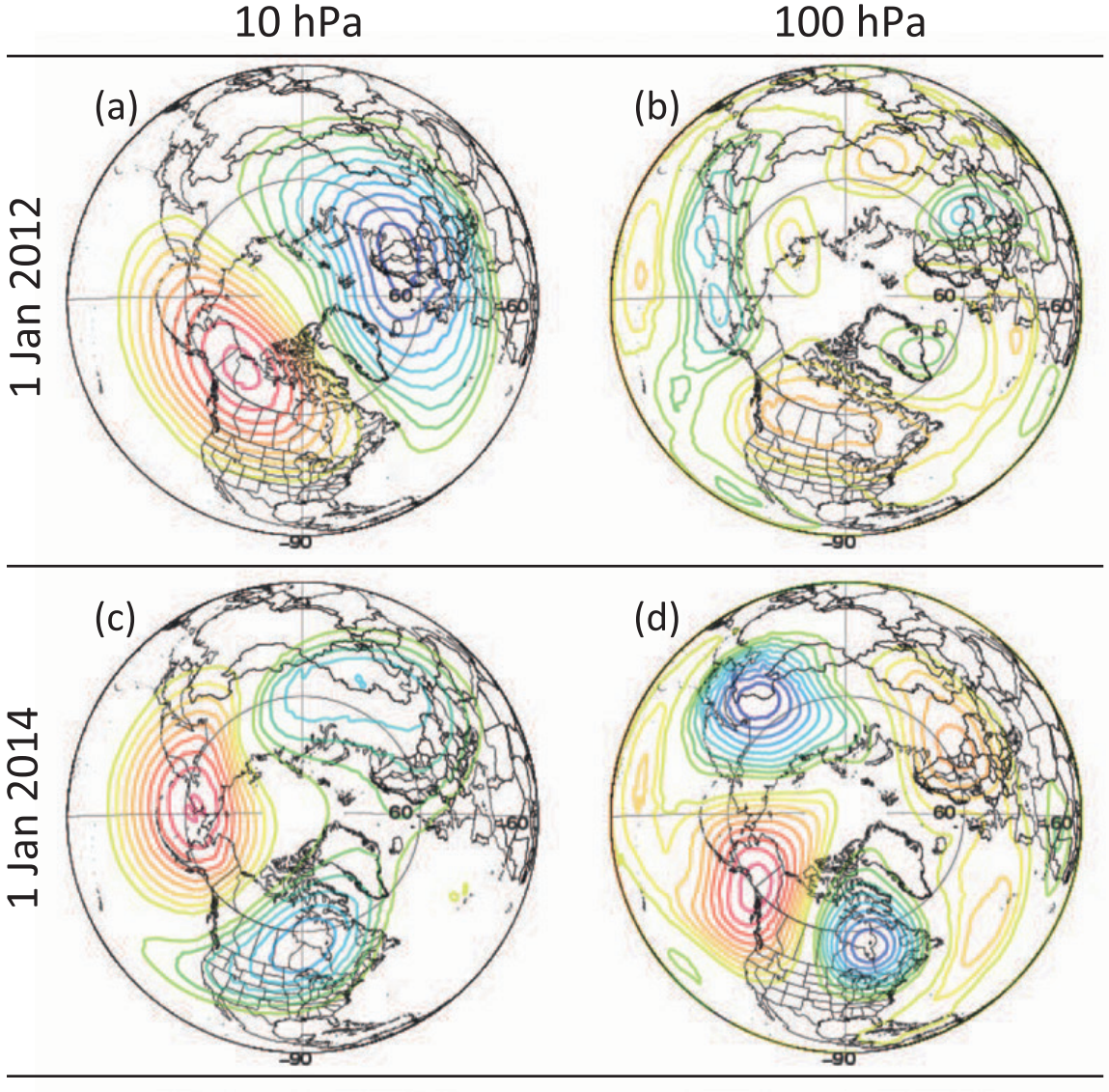

Fig. 4. The departure from GFS analysis zonal-mean geopotential height on 1 Jan 2012 at (a) 10 hPa, every 150 m, and (b) 100 hPa, every 50 m, as well as on 1 Jan 2014 at (c) 10 hPa, every 150 m, and (d) 100 hPa, every 50 m. The 60°N latitude circle represents the characteristic polar vortex edge.

different spatial wave structures in the stratosphere (Fig. 4). The stratospheric pattern was predominantly wavenumber 1 in early January 2012 (Figs. 4a,b), whereas it was closer to wavenumber 2 in January 2014 (Figs. 4c,d). Comparing Figs. 2 and 4 illustrates that anomalous 500-hPa geopotential height anomalies over North America in both winters were connected with similar anomalies in the stratosphere. For example, the anomalous 500-hPa trough over the Midwest–East responsible for the cold winter of 2013/14 (Fig. 2b) extended upward and linked to the wavenumber-2 structure in the stratospheric polar vortex (Figs. 4c,d).

The areal extent of snow cover over Eurasia (Robinson et al. 1993) represents another source of predictability for the AO/NAO. Above-normal Eurasian snow cover in October can lead to a more negative AO/NAO throughout the winter (Cohen and Entekhabi 1999; Cohen et al. 2010; Cohen and Jones 2011; Smith et al. 2011). The enhanced Eurasian snow strengthens the Siberian high, and these anomalies may propagate vertically into the stratosphere where they have more lasting effects on the AO/NAO.

TROPICAL TELECONNECTIONS. ENSO is an important tool for seasonal temperature forecasting. El Niño events are typically associated with warm winter temperatures in the Midwest–East region, whereas La Niña winters are generally cooler than normal (Ropelewski and Halpert 1986; Harrison and Larkin 1998; Higgins et al. 2002; Chiodi and Harrison 2013). The warm signals over North America primarily occur with conventional eastern Pacific warming events and less frequently with central Pacific warming events (Larkin and Harrison 2005; Weng et al. 2009; Chiodi and Harrison 2013).

Just as ENSO is the leading mode of tropical interannual variability, the MJO is the leading mode on intraseasonal time scales. The MJO moves eastward in the tropics with a period of 30–60 days (Zhang 2005), and its tropical convection interacts with circulations around the globe, including weather patterns over North America (Becker et al. 2011; Zhou et al. 2012; Riddle et al. 2013; Johnson and Feldstein 2010; Schreck et al. 2013; Zhang 2013). Dynamical models are only just beginning to tap the long-range predictability of the MJO (Gottschalck et al. 2010; Weaver et al. 2011), so it represents a key opportunity for human forecasts to improve upon those from the models. The MJO's 30–60-day period lends itself to the analog methods that many energy meteorologists use for long-range forecasting. They predict the evolution of the MJO on Wheeler and Hendon's (2004) real-time multivariate MJO (RMM) index and then extrapolate Midwest–East temperatures based on composites for each of the RMM's eight phases. Those temperatures tend to be warmer in the 6–10 days following phases 3–5 and cooler following phase 8 (Zhou et al. 2012; Schreck et al. 2013). The RMM index can be sensitive to higher-frequency equatorial waves (Roundy et al. 2009), so forecasters often complement the index by examining Hovmöller diagrams

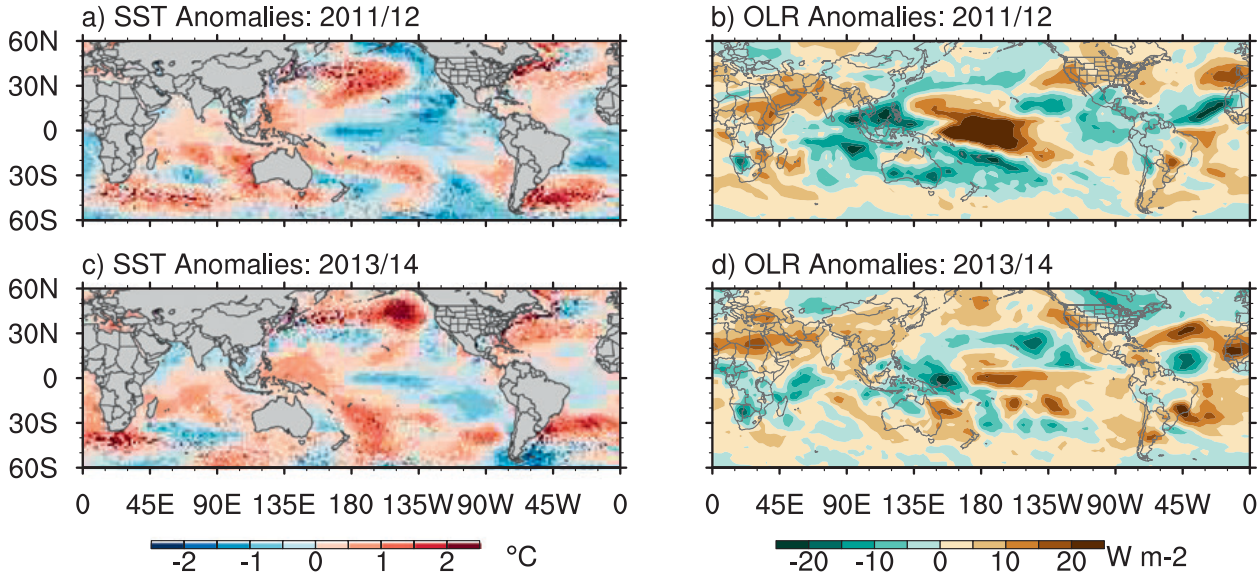

Fig. 5. Dec–Feb anomalies relative to 1981–2010 of (a),(c) optimum interpolation (OI) SST (Reynolds et al. 2007; Reynolds 2009; Banzon and Reynolds 2013) and (b),(d) High Resolution Infrared Radiation Sounder (HIRS) OLR (Lee et al. 2007) for (top) 2011/12 and (bottom) 2013/14.

of daily OLR anomalies (Wheeler and Weickmann 2001; Liebmann and Smith 1996; Lee 2014).

Figure 5 shows global maps of sea surface temperatures (SSTs; Reynolds et al. 2007; Reynolds 2009; Banzon and Reynolds 2013) and outgoing longwave radiation (OLR; Lee et al. 2007), two fields that energy meteorologists use to identify tropical forcing for Midwest–East temperatures. They are particularly concerned with the SST patterns over the tropical Pacific, which define the characteristics of the ENSO state more than any single index (e.g., Fig. 8a) (Trenberth 1997). OLR is similarly important for identifying variability in tropical convection, which acts as a bridge between the SSTs and Midwest–East temperatures (Chiodi and Harrison 2013).

The winters of 2011/12 and 2013/14 both featured cooler-than-normal SSTs in the equatorial central Pacific coincident with positive OLR anomalies that indicate atmospheric subsidence (Fig. 5). These features were stronger in 2011/12 and extended farther into the western Pacific. The enhanced convection near the South China Sea in 2011/12 and the accompanying upper-tropospheric outflow could have played a role in the extended Pacific jet seen in Fig. 2a (Kiladis and Weickmann 1992; Matthews et al. 2004; Johnson and Feldstein 2010). Similarly, the enhanced convection in the western Pacific during 2013/14 was consistent with the more amplified flow that winter.

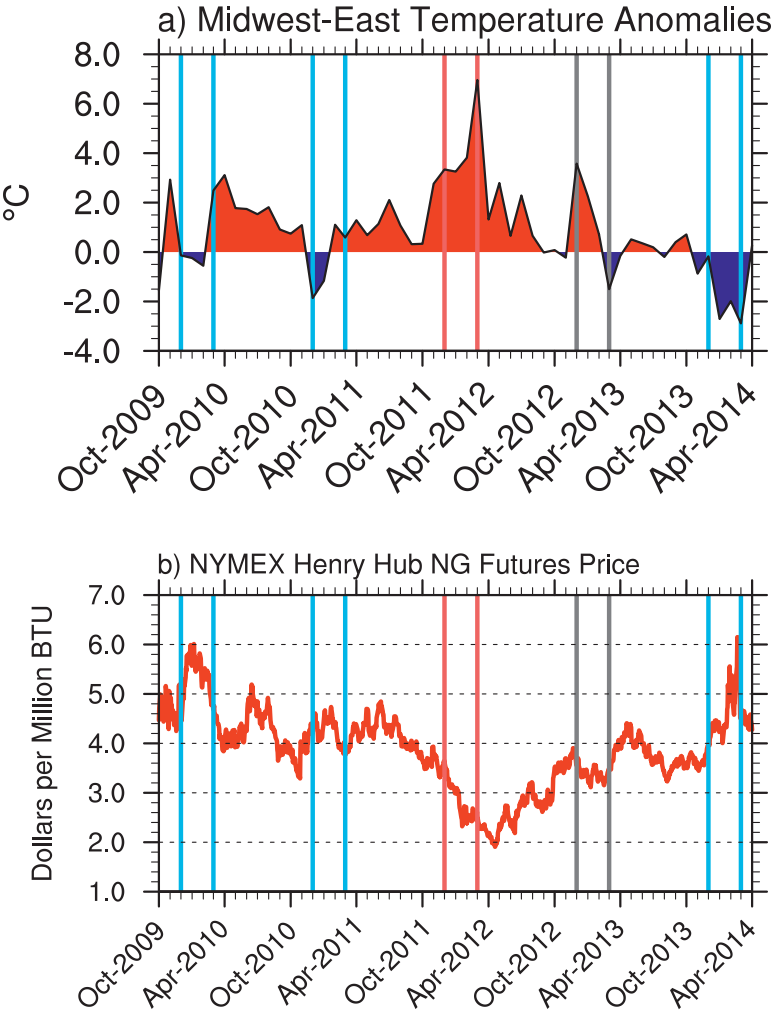

Fig. 6. Time series of (a) monthly temperature anomalies relative to 1981–2010 averaged over the Midwest–East region and (b) daily Henry Hub natural gas futures prices. Vertical lines denote Dec–Feb seasons that were cold (blue), warm (red), or neutral (gray).

Another unique feature in 2013/14 was the unusually warm (>2.5°C) SST anomalies in the Gulf of Alaska (Fig. 5c). These SSTs were more than 1.0°C warmer than any previously experienced in that region during December–February since the satellite record began in 1981/82. Previous studies have generally concluded that North Pacific SST anomalies are driven largely by the local atmospheric circulation (Davis 1976; Cayan 1992; Liu et al. 2006). However, the SST anomalies can in turn affect the atmospheric circulation by forcing a Pacific–North America (PNA) like pattern and an enhanced ridge over the Gulf of Alaska similar to that seen in Fig. 2b (Peng and Whitaker 1999; Liu et al. 2006; Frankignoul and Sennéchael 2007).

FLUCTUATING TEMPERATURES, SUPPLY, AND DEMAND. *Warmth and surpluses in 2011/12.* Figure 6 shows the evolution of Midwest–East temperature anomalies and the Henry Hub natural gas futures price since 2009. The temperature data in this study originate from a subset of the Global Historical Climatology Network-Daily (GHCN-D) dataset (Menne et al. 2012), which is currently used in the National Oceanic and Atmospheric Administration/National Centers for Environmental Information (NOAA/NCEI) climate division dataset (Vose et al. 2014). For most of 2009–11, prices fluctuated steadily around \$3.00–\$5.00 mmBTU^{-1} (Fig. 6b). They had fallen precipitously since their record high

of $13.58 mmBTU^{-1} on 3 July 2008 as a result of the combination of increased supply from high-volume hydraulic fracturing in the Marcellus Shale and a generally weak macroeconomy. During the 2011/12, natural gas prices fell steadily from $4.85 mmBTU^{-1} on 8 June 2011 to an 11-yr low of $1.91 mmBTU^{-1} on 19 April 2012. This drop of 61% in 10 months included an unusually warm winter that squelched demand (Fig. 6b). Midwest–East temperatures were 3.5°C above the 1981–2010 normal for December–February, culminating in an unprecedented anomaly of +7.0°C during March 2012.

Figure 7a shows the distribution of temperature anomalies relative to their twentieth-century climatology by state for December–February 2011/12. Every state had above-normal temperatures, and 2011/12 was the third warmest December–February nationwide in 119 years of records (Vose et al. 2014). More than 20 states from Montana to Maine had one of their 10 warmest winters on record. The largest temperature anomalies were concentrated in the Midwest and northeastern United States, which explains the large impact of this warmth on natural gas prices.

Figure 8 shows the evolution of some of the key teleconnection indices in recent years. Winter 2011/12 demonstrated the limitations of using ENSO for seasonal forecasting. La Niña during 2011/12 (Figs. 5a and 8a) would have suggested cooler Midwest–East temperatures, but instead those temperatures were exceptionally warm. This disconnect from the expected La Niña impacts suggests that higher-latitude signals may have overwhelmed the ENSO signal. Eurasian snow cover was below normal until November (Fig. 8b), which may have played a role in the positive AO/NAO (Figs. 8c,d) and subsequent warm Midwest–East temperatures that winter. Interestingly, Midwest–East temperatures remained above normal even after the SSW in January 2012 (Fig. 3) and the subsequent switch to negative AO (Fig. 8c).

Figure 9 shows the annual cycle of natural gas storage for the last 20 years. Storage increases during the summer months and then that stored gas is consumed during the winter. Reserves of natural gas were already above normal in June of 2011 (red line). Natural gas production has been

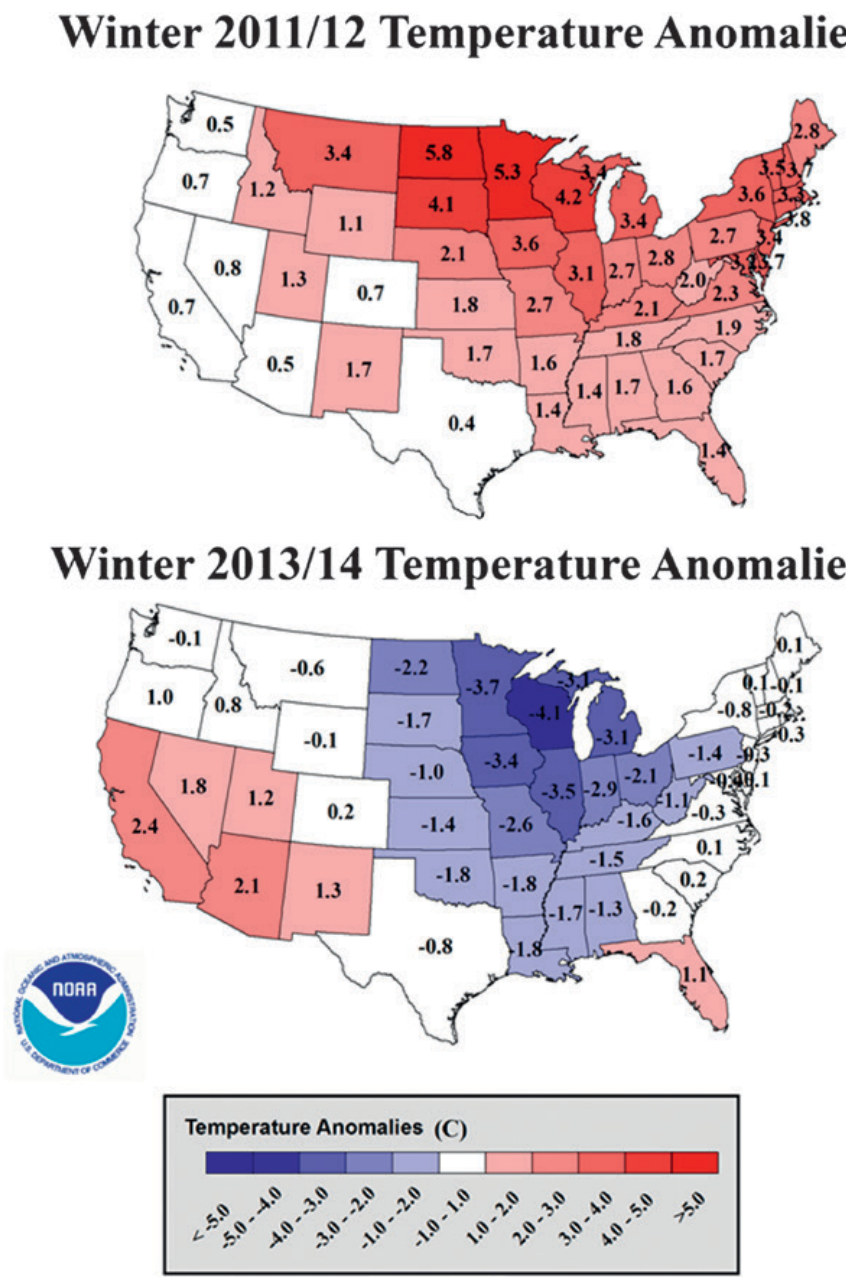

Fig. 7. Statewide Dec–Feb temperature anomalies from their twentieth-century averages for (a) 2011/12 and (b) 2013/14.

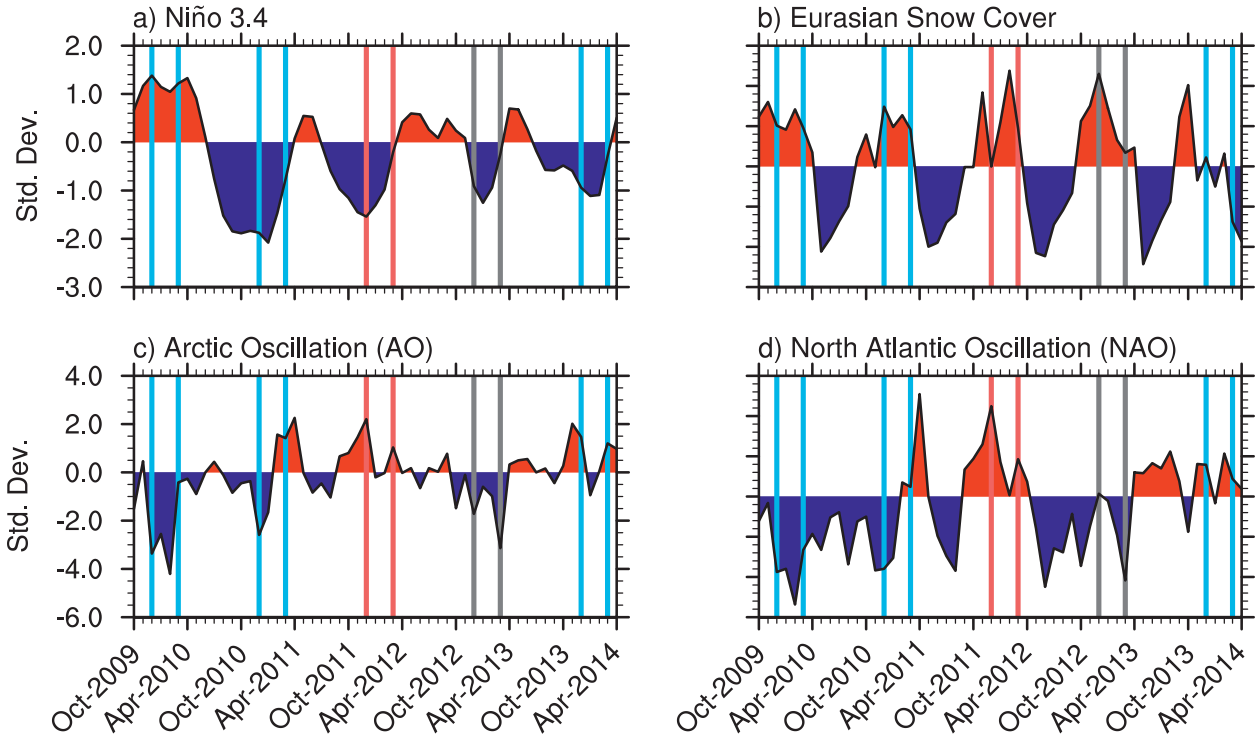

Fig. 8. Monthly standardized anomalies relative to 1981–2010 of the (a) Niño-3.4, (b) Eurasian snow cover, (c) AO, and (d) NAO. Vertical lines are as in Fig. 6.

steadily increasing in recent years with the advent of high-volume hydraulic fracturing in the Marcellus Shale (Turcotte et al. 2014). Producers further increased supply in 2011 to prepare for the possibility of another cold winter with above-normal demand, as in the years 2009/10 and 2010/11. Instead, the extreme warmth suppressed demand in 2011/12. Natural gas storage attained record seasonal levels from December 2011 through April 2012, which pushed prices downward.

Unusual heat and sensitivity in March 2012. March 2012 was exceptional both for its temperatures over the United States and their impacts on the natural gas markets. March is usually a time when energy traders pay less attention to the weather. Temperatures are generally milder during early spring (Arguez et al. 2012), so it is a relative lull in heating and cooling demand. Many power plants use early spring for maintenance, and these maintenance schedules dominate the supply and demand balances. Since humans drive these schedules, traders have less clarity in the market fundamentals and many of them will limit their exposure during this season. However, the warmth in March 2012 was so extreme that even the minimal amount of heating demand typically associated with the month did not materialize. The natural gas markets continued to plunge downward, eventually reaching an 11-yr low of \$1.91 mmBTU^{-1} on 19 April.

The contiguous United States was 4.95°C above its twentieth-century average for March 2012 (3.2 standard deviations above normal). It was the largest positive anomaly for any month since records began in 1895. During the course of the month, over 15,000 warm temperature records were broken at the station level. Numerous stations even had daily minimum (nighttime) temperatures that exceeded the previous daily maximum (daytime) temperature records for the same date. Figure 10 shows the temperature anomalies by state for March 2012. Except for the Pacific coast, every state was above their twentieth-century mean, and 31 states experienced their warmest March on record. The warmth was particularly strong in the Midwest–East region where 10 states were at least 8°C above normal.

A high-amplitude MJO event played a major role in this warmth (Dole et al. 2014). Figure 11a shows the evolution of the RMM index during this event that developed in early February 2012 and continued throughout March (Gottschalck et al. 2013). The first half of March was spent in phases 3–5, which favor warmer Midwest–East temperatures. Schreck et al. (2013) recently showed that the MJO's impacts on North American temperatures depend in part on the preexisting extratropical circulation. To diagnose these effects, they developed the multivariate Pacific–North America (MVP) index (Fig. 11b). When

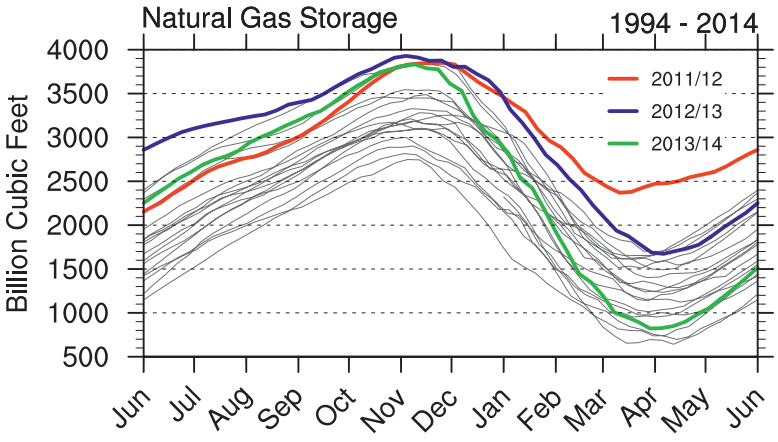

Fig. 9. Seasonal cycle of weekly natural gas in underground storage for each year from 1994/95 to 2013/14.

this index is negative, as it was during most of March 2012, the MJO has an even larger warming effect on Midwest–East temperatures. Figure 11 suggests that both the tropics and extratropics were well positioned to yield the extreme warmth that was observed in March 2012, as discussed in greater detail by Dole et al. (2014).

Cold and depletion in 2013/14. Natural gas prices remained volatile but gradually recovered during 2012 and 2013 as temperatures remained closer to normal and the surplus gas was consumed (Figs. 6 and 9). However, the winter of 2013/14 sent another shock to the markets. Temperatures were 1.6°C below their twentieth-century normal for Midwest–East in December–February. The coldest temperatures were focused on the Midwest (Fig. 7b), with seven states having 1 of their 10 coldest winter seasons. Wisconsin bore the brunt of the cold. The statewide average temperature for December–February 2013/14 was 4.0°C below the twentieth-century average. It was the coldest winter for Wisconsin since 1978/79 and the fifth coldest on record. In addition to the cold temperatures, New York, New York; Philadelphia, Pennsylvania; Chicago; and Boston all had 1 of their 10 snowiest winters on record, with Detroit, Michigan, breaking its December–February snowfall record.

ENSO was neutral in 2013/14 (Fig. 8a), which limited the skill of forecasts going into the season. Eurasian snow cover was above normal in September and October (Fig. 8b), which would favor a negative AO/NAO and cold Midwest–East temperatures. The cold temperatures materialized (Fig. 6a) even though the negative AO/NAO did not (Fig. 8c,d). The widespread cold in 2013/14 drove up natural gas prices and exhausted the surpluses of storage (Figs. 6b and 9). Natural gas storage plummeted from the fifth highest in the 21-yr record in November 2013 to fourth lowest in April 2014 (Fig. 9). Concerns about potential natural gas shortages (Friedman 2014) drove the Henry Hub futures price up 141% from \$3.45 mmBTU^{-1} on 4 November 2013 to \$6.15 mmBTU^{-1} on 19 February 2014, the highest price since before the macroeconomic crash in 2008.

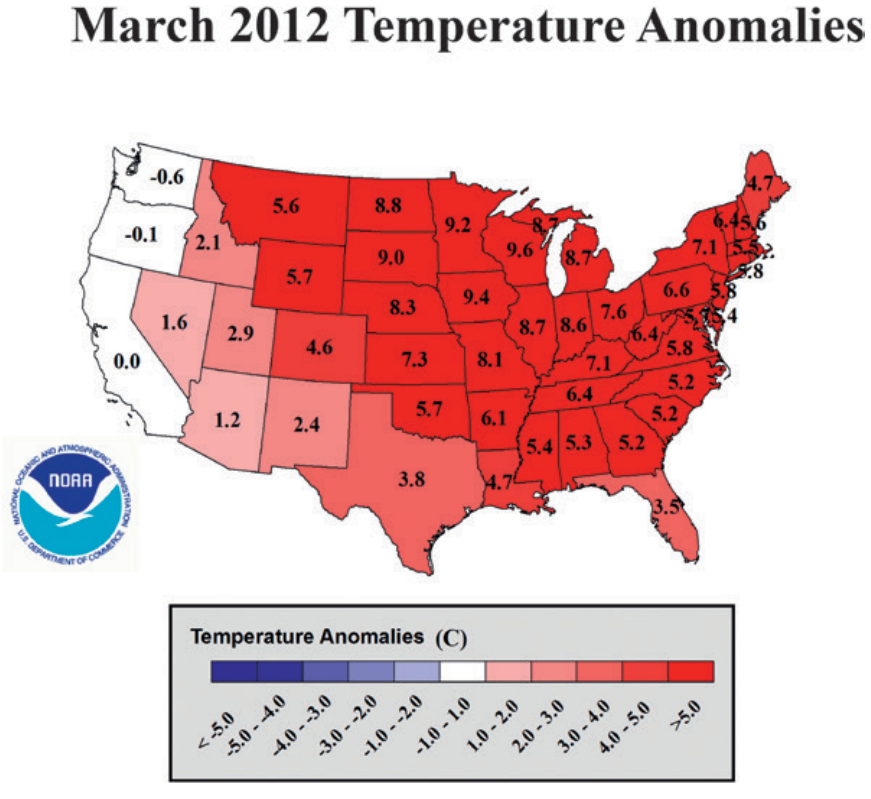

Fig. 10. As in Fig. 7, but for Mar 2012.

Markets and models. One example of the market's reaction to the models happened on Tuesday, 31 December 2013. While the markets were closed over the previous weekend, the ECMWF ensemble trended substantially warmer in its 11–15-day forecasts. Figure 12 shows changes of more than 10°F (5.6°C) for portions of the Midwest–East region compared with the previous forecast. The market remained stable on Monday as the GFS continued to predict a colder solution. However, the 1200 UTC GFS forecast from Tuesday, 31 December, demonstrated a shift toward warmer temperatures (not shown) similar to the one observed in the ECMWF forecasts a few days earlier (Fig. 12). This prompted the larger weather vendors, including Weather Services International (WSI) and EarthSat, to issue warmer outlooks. This consensus on a warmer forecast for week 2 triggered a selloff. Natural gas futures contracts for February (NGG4) declined from an opening of $4.43 to $4.23 mmBTU^{-1} at closing, resulting in a 4.4% loss in a single day (Malik 2013). If a trader had foreknowledge that the forecast would continue trending warmer, they could have sold their natural gas holdings ahead of this decline.

The warmer forecast was accurate, with warmer temperatures suppressing demand during an otherwise cold winter in 2013/14. The shift toward warmer forecasts coincided with a sharp increase in wave propagation upward into the stratosphere (not shown). Resolving this upward surge in wave activity may have improved the models' initialization of the stratospheric circulation and enabled them to identify this warmer solution (Charlton et al. 2004; Jung and Barkmeijer 2006; Roff et al. 2011; Gerber et al. 2012).

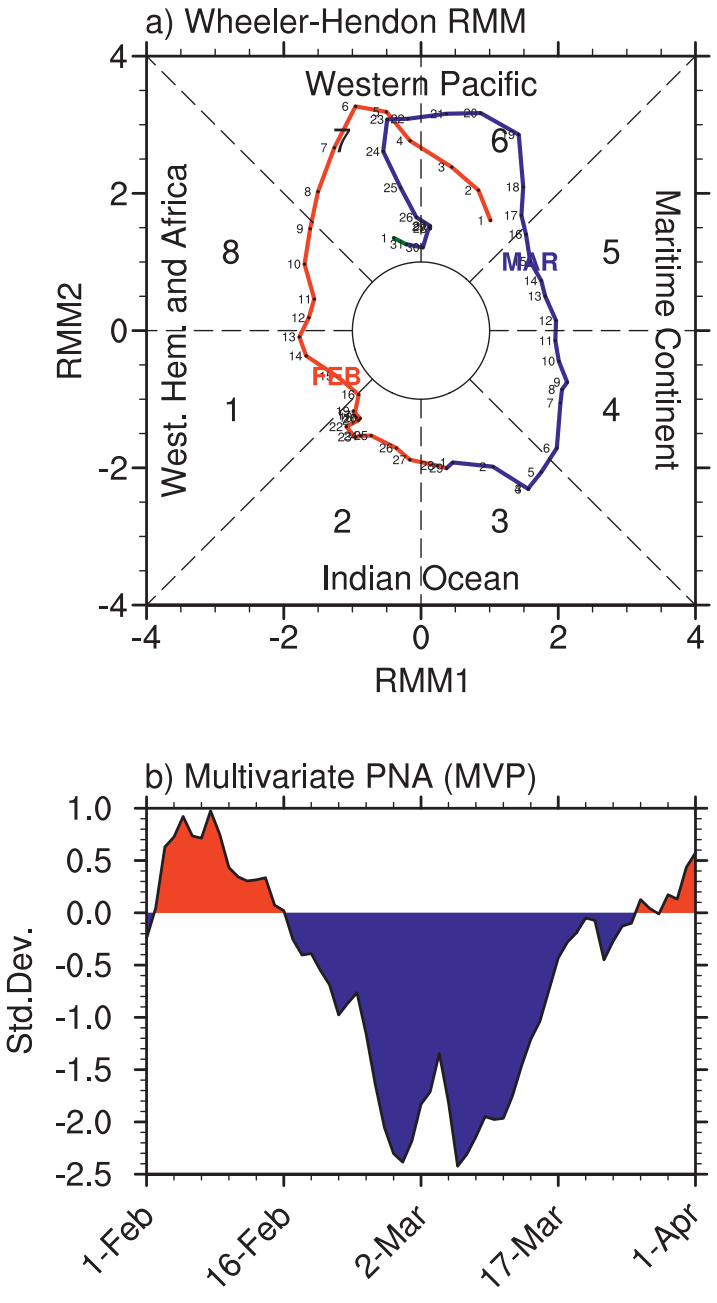

Fig. 11. (a) The Wheeler and Hendon (2004) RMM index and (b) MVP index for Feb–Mar 2012.

SUMMARY. This study used the extreme winters of 2011/12 and 2013/14 to examine the use of weather and climate data in the natural gas markets. While natural gas prices fluctuate with variations in both supply and demand, the events presented here were driven largely by demand related to temperatures over the northeastern quadrant of the United States (Midwest–East; Fig. 1). These linkages were apparent as prices fell during the extremely warm winter of 2011/12 and then rose again during the cold winter of 2013/14.

Energy companies trade monthly futures contracts to hedge their risk against these weather-driven fluctuations, as well as to speculate and increase their overall profitability. Everyone in the market has roughly equal access to guidance from dynamical models, so the market reacts strongly to changes in these forecasts. Traders look to energy meteorologists and weather vendors to provide them with long-range temperature forecasts that can improve upon

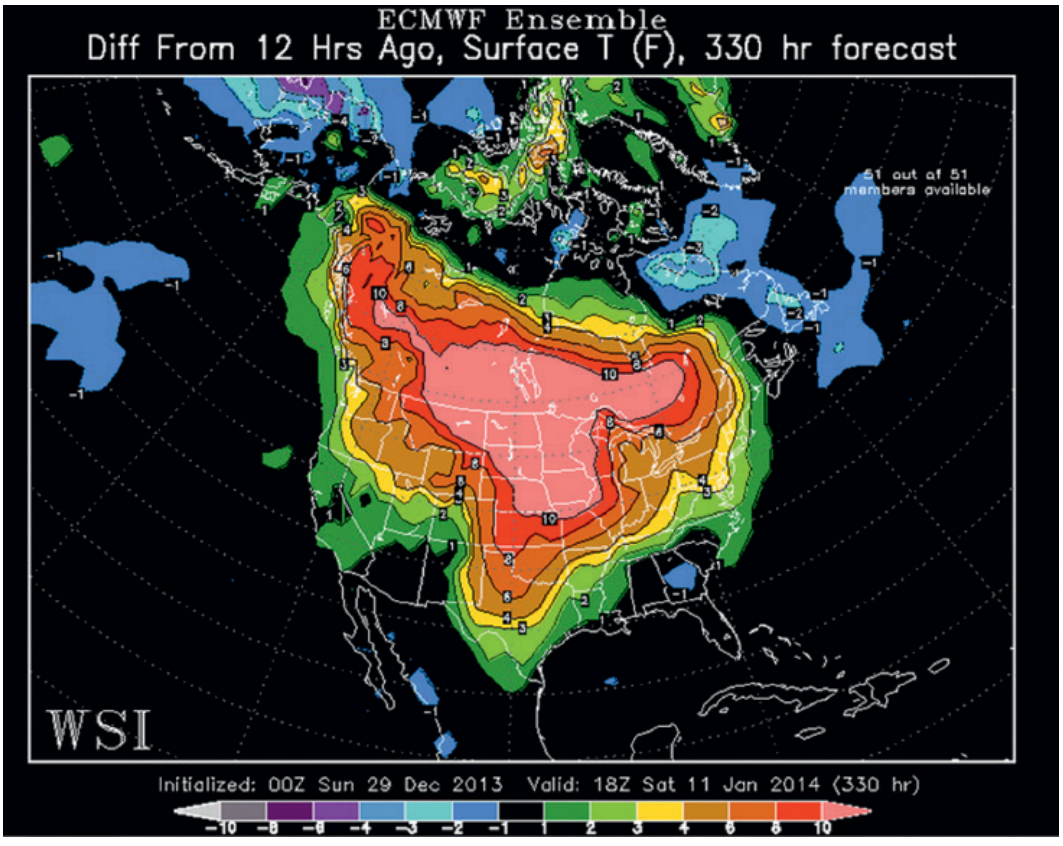

Fig. 12. Difference in forecast surface temperatures valid at 1800 UTC 11 Jan 2014 between ECWMF ensemble runs initialized at 0000 UTC 29 Dec and 1200 UTC 28 Dec 2013.

the models. These forecasts often rely on historical analogs based on teleconnection indices in the tropics and the Arctic. In this study, we examined how the markets and those teleconnections evolved during 2011/12 and 2013/14.

Winter 2011/12 was exceptionally warm (Fig. 7a), which suppressed natural gas demand. Combined with increased natural gas production, the lack of demand led to record surpluses in natural gas storage (Fig. 9) and sharp declines in prices (Fig. 6b). The warmth in 2011/12 was consistent with a classic positive AO pattern (Fig. 2a). That pattern was dominated by zonal flow around the Northern Hemisphere and an elongated Pacific jet that minimized the opportunities for cold-air outbreaks into the United States. The stratospheric vortex broke down in the first week of January 2012 (Fig. 3a), linked to a weakening of the positive AO (Fig. 8c). The warmth in the Midwest–East continued and even intensified in association with intraseasonal and synoptic-scale features, including an unusually strong MJO (Fig. 11) (Dole et al. 2014). As a result, March 2012 was the most anomalously warm month on record for the United States since 1895. Natural gas prices are usually more stable during March, but this extreme anomaly drove prices down to an 11-yr low.

Winter 2013/14 presented a sharp contrast to 2011/12, as Midwest–East temperatures were anomalously cold (Fig. 7b). The resulting demand consumed the remaining surplus of natural gas inventory (Fig. 9) and drove prices upward (Fig. 6b). The cold in 2013/14 emanated from a Northern Hemisphere pattern dominated by anomalous ridging over the Gulf of Alaska (Fig. 2b). The ridge extended all the way to the pole and transported cold air from Siberia to North America. This ridge and the downstream trough over North America were both vertically deep features that were linked with a wavenumber-2 pattern in the stratospheric polar vortex (Figs. 2b and 4c,d). The resulting cold temperatures quickly led natural gas prices upward to their highest levels in 6 yr (Figs. 6b and 9).

The fluctuations in natural gas prices during the extreme winters of 2011/12 and 2013/14 underscore the susceptibility of our economy to ever-changing weather patterns. Continuing improvements to long-range forecasts will increase the efficiency of our energy markets. Ongoing advancements in numerical

weather prediction are an obvious avenue for such improvements. Another would be developing new analog methods to harness the increasing number of long-term homogenized satellite climate data records (National Research Council 2004). Both pathways would enable energy companies to plan and adapt more quickly to future extremes.

ACKNOWLEDGMENTS. This study was inspired by the Executive Forum on Business and Climate supported by the Cooperative Institute for Climate and Satellites—North Carolina (CICS—NC) and NOAA's National Centers for Environmental Information in June 2013. The manuscript benefited significantly from the comments of two anonymous reviewers. Schreck received support for this research from NOAA's Climate Data Record (CDR) program through CICS–NC under Cooperative Agreement NA14NES432003. Natural gas prices and storage data were provided by the Energy Information Administration. Niño-3.4, AO, and NAO are calculated by NOAA/CPC and obtained from NOAA/ESRL/PSD. Eurasian snow cover was obtained from the Rutgers Snow Lab.

REFERENCES

Ambaum, M. H. P., B. J. Hoskins, and D. B. Stephenson, 2001: Arctic Oscillation or North Atlantic Oscillation? *J. Climate,* **14,** 3495–3507, doi:10.1175/1520-0442(2001)014<3495:AOONAO>2.0.CO;2.

Arguez, A., I. Durre, S. Applequist, R. S. Vose, M. F. Squires, X. Yin, R. R. Heim, and T. W. Owen, 2012: NOAA's 1981–2010 U.S. climate normals: An overview. *Bull. Amer. Meteor. Soc.,* **93,** 1687–1697, doi:10.1175/BAMS-D-11-00197.1.

Baldwin, M. P., and T. J. Dunkerton, 1999: Propagation of the Arctic Oscillation from the stratosphere to the troposphere. *J. Geophys. Res.,* **104,** 30 937–30 946, doi:10.1029/1999JD900445.

——, and ——, 2001: Stratospheric harbingers of anomalous weather regimes. *Science,* **294,** 581–584, doi:10.1126/science.1063315.

——, D. B. Stephenson, D. W. J. Thompson, T. J. Dunkerton, A. J. Charlton, and A. O'Neill, 2003: Stratospheric memory and skill of extended-range weather forecasts. *Science,* **301,** 636–640, doi:10.1126/science.1087143.

Banzon, V. F., and R. W. Reynolds, 2013: Use of WindSat to extend a microwave-based daily optimum interpolation sea surface temperature time series. *J. Climate,* **26,** 2557–2562, doi:10.1175/JCLI-D-12-00628.1.

Barnston, A. G., and R. E. Livezey, 1987: Classification, seasonality and persistence of low-frequency atmospheric circulation patterns. *Mon. Wea. Rev.,* **115,** 1083–1126, doi:10.1175/1520-0493(1987)115<1083:CSAPOL>2.0.CO;2.

Becker, E. J., E. H. Berbery, and R. W. Higgins, 2011: Modulation of cold-season U.S. daily precipitation by the Madden–Julian oscillation. *J. Climate,* **24,** 5157–5166, doi:10.1175/2011JCLI4018.1.

Black, R. X., 2002: Stratospheric forcing of surface climate in the Arctic Oscillation. *J. Climate,* **15,** 268–277, doi:10.1175/1520-0442(2002)015<0268:SFOSCI>2.0.CO;2.

Brown, S. P. A., and M. K. Yücel, 2008: What drives natural gas prices? *Energy J.,* **29,** 45–60.

Cayan, D. R., 1992: Latent and sensible heat flux anomalies over the northern oceans: Driving the sea surface temperature. *J. Phys. Oceanogr.,* **22,** 859–881, doi:10.1175/1520-0485(1992)022<0859:LASHFA>2.0.CO;2.

Charlton, A. J., A. O'neill, W. A. Lahoz, and A. C. Massacand, 2004: Sensitivity of tropospheric forecasts to stratospheric initial conditions. *Quart. J. Roy. Meteor. Soc.,* **130,** 1771–1792, doi:10.1256/qj.03.167.

Chiodi, A. M., and D. E. Harrison, 2013: El Niño impacts on seasonal U.S. atmospheric circulation, temperature, and precipitation anomalies: The OLR-event perspective. *J. Climate,* **26,** 822–837, doi:10.1175/JCLI-D-12-00097.1.

Cohen, J., and D. Entekhabi, 1999: Eurasian snow cover variability and Northern Hemisphere climate predictability. *Geophys. Res. Lett.,* **26,** 345–348, doi:10.1029/1998GL900321.

——, and J. Jones, 2011: A new index for more accurate winter predictions. *Geophys. Res. Lett.,* **38,** L21701, doi:10.1029/2011GL049626.

——, J. Foster, M. Barlow, K. Saito, and J. Jones, 2010: Winter 2009–2010: A case study of an extreme Arctic Oscillation event. *Geophys. Res. Lett.,* **37,** L17707, doi:10.1029/2010GL044256.

Davis, R. E., 1976: Predictability of sea surface temperature and sea level pressure anomalies over the North Pacific Ocean. *J. Phys. Oceanogr.,* **6,** 249–266, doi:10.1175/1520-0485(1976)006<0249:POSSTA>2.0.CO;2.

Dole, R., and Coauthors, 2014: The making of an extreme event: Putting the pieces together. *Bull. Amer. Meteor. Soc.,* **95,** 427–440, doi:10.1175/BAMS-D-12-00069.1.

Frankignoul, C., and N. Sennéchael, 2007: Observed influence of North Pacific SST anomalies on the atmospheric circulation. *J. Climate,* **20,** 592–606, doi:10.1175/JCLI4021.1.

Friedman, N., 2014: Natural gas soars as stockpiles drop. *Wall Street Journal,* 13 February, accessed 30 May 2014. [Available online at http://online.wsj.com

/news/articles/SB10001424052702304888404579380732212718914.]

Gerber, E. P., and Coauthors, 2012: Assessing and understanding the impact of stratospheric dynamics and variability on the Earth system. *Bull. Amer. Meteor. Soc.,* **93,** 845–859, doi:10.1175/BAMS-D-11-00145.1.

Gottschalck, J., and Coauthors, 2010: A framework for assessing operational Madden–Julian oscillation forecasts: A CLIVAR MJO Working Group project. *Bull. Amer. Meteor. Soc.,* **91,** 1247–1258, doi:10.1175/2010BAMS2816.1.

——, P. E. Roundy, C. J. Schreck III, A. Vintzileos, and C. Zhang, 2013: Large-scale atmospheric and oceanic conditions during the 2011–12 DYNAMO field campaign. *Mon. Wea. Rev.,* **141,** 4173–4196, doi:10.1175/MWR-D-13-00022.1.

Hagedorn, R., T. M. Hamill, and J. S. Whitaker, 2008: Probabilistic forecast calibration using ECMWF and GFS ensemble reforecasts. Part I: Two-meter temperatures. *Mon. Wea. Rev.,* **136,** 2608–2619, doi:10.1175/2007MWR2410.1.

Harrison, D. E., and N. K. Larkin, 1998: Seasonal U.S. temperature and precipitation anomalies associated with El Niño: Historical results and comparison with 1997-98. *Geophys. Res. Lett.,* **25,** 3959–3962, doi:10.1029/1998GL900061.

Higgins, R. W., A. Leetmaa, Y. Xue, and A. Barnston, 2000: Dominant factors influencing the seasonal predictability of U.S. precipitation and surface air temperature. *J. Climate,* **13,** 3994–4017, doi:10.1175/1520-0442(2000)013<3994:DFITSP>2.0.CO;2.

——, ——, and V. E. Kousky, 2002: Relationships between climate variability and winter temperature extremes in the United States. *J. Climate,* **15,** 1555–1572, doi:10.1175/1520-0442(2002)015<1555:RBCVAW>2.0.CO;2.

Hurrell, J. W., Y. Kushnir, G. Ottersen, and M. Visbeck, 2003: An overview of the North Atlantic oscillation. *The North Atlantic Oscillation: Climatic Significance and Environmental Impact*, J. W. Hurrell et al., Amer. Geophys. Union, 1–35.

Joëts, M., and V. Mignon, 2012: On the link between forward energy prices: A nonlinear panel cointegration approach. *Energy Econ.,* **34,** 1170–1175, doi:10.1016/j.eneco.2011.10.019.

Johnson, N. C., and S. B. Feldstein, 2010: The continuum of North Pacific sea level pressure patterns: Intraseasonal, interannual, and interdecadal variability. *J. Climate,* **23,** 851–867, doi:10.1175/2009JCLI3099.1.

Jung, T., and J. Barkmeijer, 2006: Sensitivity of the tropospheric circulation to changes in the strength of the stratospheric polar vortex. *Mon. Wea. Rev.,* **134,** 2191–2207, doi:10.1175/MWR3178.1.

Kanamitsu, M., W. Ebisuzaki, J. Woollen, S.-K. Yang, J. J. Hnilo, M. Fiorino, and G. L. Potter, 2002: NCEP–DOE AMIP-II Reanalysis (R-2). *Bull. Amer. Meteor. Soc.,* **83,** 1631–1643, doi:10.1175/BAMS-83-11-1631.

Kiladis, G. N., and K. M. Weickmann, 1992: Circulation anomalies associated with tropical convection during northern winter. *Mon. Wea. Rev.,* **120,** 1900–1923, doi:10.1175/1520-0493(1992)120<1900:CAAWTC>2.0.CO;2.

Labitzke, K., 1972: Temperature changes in the mesosphere and stratosphere connected with circulation changes in winter. *J. Atmos. Sci.,* **29,** 756–766, doi:10.1175/1520-0469(1972)029<0756:TCITMA>2.0.CO;2.

Larkin, N. K., and D. E. Harrison, 2005: On the definition of El Niño and associated seasonal average U.S. weather anomalies. *Geophys. Res. Lett.,* **32,** L13705, doi:10.1029/2005GL022738.

Lee, H.-T., 2014: Climate Algorithm Theoretical Basis Document (C-ATBD): Outgoing longwave radiation (OLR) - Daily. Climate Data Record Program Rep. CDRP-ATBD-0526, NOAA/NCDC, 46 pp. [Available online at http://www1.ncdc.noaa.gov/pub/data/sds/cdr/CDRs/Outgoing%20Longwave%20Radiation%20-%20Daily/AlgorithmDescription.pdf.]

——, A. Gruber, R. G. Ellingson, and I. Laszlo, 2007: Development of the HIRS outgoing longwave radiation climate dataset. *J. Atmos. Oceanic Technol.,* **24,** 2029–2047, doi:10.1175/2007JTECHA989.1.

Liebmann, B., and C. A. Smith, 1996: Description of a complete (interpolated) outgoing longwave radiation dataset. *Bull. Amer. Meteor. Soc.,* **77,** 1275–1277.

Linn, S. C., and Z. Zhu, 2004: Natural gas prices and the gas storage report: Public news and volatility in energy futures markets. *J. Futures Mark.,* **24,** 283–313, doi:10.1002/fut.10115.

Liu, Q., N. Wen, and Z. Liu, 2006: An observational study of the impact of the North Pacific SST on the atmosphere. *Geophys. Res. Lett.,* **33,** L18611, doi:10.1029/2006GL026082.

Malik, N. S., 2013: Natural gas trims biggest annual gain since 2005 as cold eases. Bloomberg.com, accessed 30 May 2014. [Available online at www.bloomberg.com/news/2013-12-31/natural-gas-rises-heads-for-biggest-annual-increase-since-2005.html.]

Matthews, A. J., B. J. Hoskins, and M. Masutani, 2004: The global response to tropical heating in the Madden–Julian oscillation during the northern winter. *Quart. J. Roy. Meteor. Soc.,* **130,** 1991–2011, doi:10.1256/qj.02.123.

Menne, M. J., I. Durre, R. S. Vose, B. E. Gleason, and T. G. Houston, 2012: An overview of the Global Historical Climatology Network-Daily database. *J. Atmos. Oceanic Technol.,* **29,** 897–910, doi:10.1175/JTECH-D-11-00103.1.

Mjelde, J. W., and D. A. Bessler, 2009: Market integration among electricity markets and their major fuel source markets. *Energy Econ.,* **31,** 482–491, doi:10.1016/j.eneco.2009.02.002.

Mu, X., 2007: Weather, storage, and natural gas price dynamics: Fundamentals and volatility. *Energy Econ.,* **29,** 46–63, doi:10.1016/j.eneco.2006.04.003.

National Research Council, 2004: *Climate Data Records from Environmental Satellites: Interim Report.* National Academies Press, 150 pp.

Newman, P. A., and J. E. Rosenfield, 1997: Stratospheric thermal damping times. *Geophys. Res. Lett.,* **24,** 433–436, doi:10.1029/96GL03720.

Novak, D. R., C. Bailey, K. F. Brill, P. Burke, W. A. Hogsett, R. Rausch, and M. Schichtel, 2014: Precipitation and temperature forecast performance at the Weather Prediction Center. *Wea. Forecasting,* **29,** 489–504, doi:10.1175/WAF-D-13-00066.1.

Peng, S., and J. S. Whitaker, 1999: Mechanisms determining the atmospheric response to midlatitude SST anomalies. *J. Climate,* **12,** 1393–1408, doi:10.1175/1520-0442(1999)012<1393:MDTART>2.0.CO;2.

Pettersson, F., P. Söderholm, and R. Lundmark, 2012: Fuel switching and climate and energy policies in the European power generation sector: A generalized Leontief model. *Energy Econ.,* **34,** 1064–1073, doi:10.1016/j.eneco.2011.09.001.

Philips, M., 2014: Northeast's record natural gas prices due to pipeline dearth. *BusinessWeek,* 6 February, accessed 6 November 2014. [Available online at www.businessweek.com/articles/2014-02-06/northeasts-record-natural-gas-prices-due-to-pipeline-dearth.]

Reynolds, R. W., 2009: What's new in version 2. NOAA/NCDC Tech. Note, 10 pp. [Available online at www.ncdc.noaa.gov/sites/default/files/attachments/Reynolds2009_oisst_daily_v02r00_version2-features.pdf.]

——, T. M. Smith, C. Liu, D. B. Chelton, K. S. Casey, and M. G. Schlax, 2007: Daily high-resolution-blended analyses for sea surface temperature. *J. Climate,* **20,** 5473–5496, doi:10.1175/2007JCLI1824.1.

Riddle, E. E., M. B. Stoner, N. C. Johnson, M. L. L'Heureux, D. C. Collins, and S. B. Feldstein, 2013: The impact of the MJO on clusters of wintertime circulation anomalies over the North American region. *Climate Dyn.,* **40,** 1749–1766, doi:10.1007/s00382-012-1493-y.

Rienecker, M. M., and Coauthors, 2011: MERRA: NASA's Modern-Era Retrospective Analysis for Research and Applications. *J. Climate,* **24,** 3624–3648, doi:10.1175/JCLI-D-11-00015.1.

Robinson, D. A., K. F. Dewey, and R. R. Heim, 1993: Global snow cover monitoring: An update. *Bull. Amer. Meteor. Soc.,* **74,** 1689–1696, doi:10.1175/1520-0477(1993)074<1689:GSCMAU>2.0.CO;2.

Roebber, P. J., and L. F. Bosart, 1996: The contributions of education and experience to forecast skill. *Wea. Forecasting,* **11,** 21–40, doi:10.1175/1520-0434(1996)011<0021:TCOEAE>2.0.CO;2.

Roff, G., D. W. J. Thompson, and H. Hendon, 2011: Does increasing model stratospheric resolution improve extended-range forecast skill? *Geophys. Res. Lett.,* **38,** L05809, doi:10.1029/2010GL046515.

Ropelewski, C. F., and M. S. Halpert, 1986: North American precipitation and temperature patterns associated with the El Niño/Southern Oscillation (ENSO). *Mon. Wea. Rev.,* **114,** 2352–2362, doi:10.1175/1520-0493(1986)114<2352:NAPATP>2.0.CO;2.

Roundy, P. E., C. J. Schreck, and M. A. Janiga, 2009: Contributions of convectively coupled equatorial Rossby waves and Kelvin waves to the real-time multivariate MJO indices. *Mon. Wea. Rev.,* **137,** 469–478, doi:10.1175/2008MWR2595.1.

Saha, S., and Coauthors, 2006: The NCEP Climate Forecast System. *J. Climate,* **19,** 3483–3517, doi:10.1175/JCLI3812.1.

——, and Coauthors, 2014: The NCEP Climate Forecast System version 2. *J. Climate,* **27,** 2185–2208, doi:10.1175/JCLI-D-12-00823.1.

Schreck, C. J., J. M. Cordeira, and D. Margolin, 2013: Which MJO events affect North American temperatures? *Mon. Wea. Rev.,* **141,** 3840–3850, doi:10.1175/MWR-D-13-00118.1.

Smith, K. L., P. J. Kushner, and J. Cohen, 2011: The role of linear interference in northern annular mode variability associated with Eurasian snow cover extent. *J. Climate,* **24,** 6185–6202, doi:10.1175/JCLI-D-11-00055.1.

Thompson, D. W. J., and J. M. Wallace, 1998: The Arctic oscillation signature in the wintertime geopotential height and temperature fields. *Geophys. Res. Lett.,* **25,** 1297–1300, doi:10.1029/98GL00950.

——, and ——, 2001: Regional climate impacts of the Northern Hemisphere annular mode. *Science,* **293,** 85–89, doi:10.1126/science.1058958.

——, M. P. Baldwin, and J. M. Wallace, 2002: Stratospheric connection to Northern Hemisphere wintertime weather: Implications for prediction. *J. Climate,* **15,**

1421–1428, doi:10.1175/1520-0442(2002)015<1421:SCTNHW>2.0.CO;2.

Trenberth, K. E., 1997: The definition of El Niño. *Bull. Amer. Meteor. Soc.,* **78,** 2771–2777, doi:10.1175/1520-0477(1997)078<2771:TDOENO>2.0.CO;2.

Tripathi, O. P., and Coauthors, 2014: The predictability of the extratropical stratosphere on monthly timescales and its impact on the skill of tropospheric forecasts. *Quart. J. Roy. Meteor. Soc.,* **141,** 987–1003 doi:10.1002/qj.2432.

Turcotte, D. L., E. M. Moores, and J. B. Rundle, 2014: Super fracking. *Phys. Today,* **67,** 34–39, doi:10.1063/PT.3.2480.

U.S. Energy Information Administration, 2012: Annual energy review 2011. DOE/EIA-0384(2011), 370 pp. [Available online at www.eia.gov/totalenergy/data/annual/pdf/aer.pdf.]

Van Oldenborgh, G. J., M. A. Balmaseda, L. Ferranti, T. N. Stockdale, and D. L. T. Anderson, 2003: Did the ECMWF seasonal forecast model outperform statistical ENSO forecast models over the last 15 years? *J. Climate,* **18,** 3240–3249, doi:10.1175/JCLI3420.1.

Vose, R. S., and Coauthors, 2014: Improved historical temperature and precipitation time series for U.S. climate divisions. *J. Appl. Meteor. Climatol.,* **53,** 1232–1251, doi:10.1175/JAMC-D-13-0248.1.

Weaver, S. J., W. Wang, M. Chen, and A. Kumar, 2011: Representation of MJO variability in the NCEP Climate Forecast System. *J. Climate,* **24,** 4676–4694, doi:10.1175/2011JCLI4188.1.

Weng, H., S. K. Behera, and T. Yamagata, 2009: Anomalous winter climate conditions in the Pacific Rim during recent El Niño Modoki and El Niño events. *Climate Dyn.,* **32,** 663–674, doi:10.1007/s00382-008-0394-6.

Wheeler, M., and K. M. Weickmann, 2001: Real-time monitoring and prediction of modes of coherent synoptic to intraseasonal tropical variability. *Mon. Wea. Rev.,* **129,** 2677–2694, doi:10.1175/1520-0493(2001)129<2677:RTMAPO>2.0.CO;2.

——, and H. H. Hendon, 2004: An all-season real-time multivariate MJO index: Development of an index for monitoring and prediction. *Mon. Wea. Rev.,* **132,** 1917–1932, doi:10.1175/1520-0493(2004)132<1917:AARMMI>2.0.CO;2.

Zhang, C., 2005: Madden-Julian oscillation. *Rev. Geophys.,* **43,** RG2003, doi:10.1029/2004RG000158.

——, 2013: Madden–Julian oscillation: Bridging weather and climate. *Bull. Amer. Meteor. Soc.,* **94,** 1849–1870, doi:10.1175/BAMS-D-12-00026.1.

Zhou, S., M. L'Heureux, S. Weaver, and A. Kumar, 2012: A composite study of the MJO influence on the surface air temperature and precipitation over the continental United States. *Climate Dyn.,* **38,** 1459–1471, doi:10.1007/s00382-011-1001-9.